Structural modification of titanium surface by octacalcium phosphate via Pulsed Laser Deposition and chemical treatment

I.V. Smirnov [a], J.V. Rau [b, **], M. Fosca [b], A. De Bonis [c], A. Latini [d], R. Teghil [c], V.I. Kalita [a], A.Yu. Fedotov [a], S.V. Gudkov [e, f, g], A.E. Baranchikov [h], V.S. Komlev [a, *]

[a] A.A. Baikov Institute of Metallurgy and Materials Science, Russian Academy of Sciences, Leninsky Prospect 49, 119334 Moscow, Russia
[b] Istituto di Struttura della Materia, Consiglio Nazionale delle Ricerche, Via del Fosso del Cavaliere 100, 00133 Rome, Italy
[c] Dipartimento di Scienze, Università della Basilicata, Viale dell'Ateneo Lucano, 10, 85100 Potenza, Italy
[d] Università di Roma "La Sapienza", Dipartimento di Chimica, Piazzale Aldo Moro, 5, 00185 Rome, Italy
[e] Lobachevsky State University, Gagarin Ave. 23, 603950 Nizhny Novgorod, Russia
[f] Prokhorov Institute of General Physics, Russian Academy of Sciences, Vavilova Street, 38, 119991 Moscow, Russia
[g] Institute of Theoretical and Experimental Biophysics, Russian Academy of Sciences, Institutskaya Street, 3, Pushchino, 142290 Moscow Region, Russia
[h] Kurnakov Institute of General and Inorganic Chemistry of the Russian Academy of Sciences, Leninsky Prospect 31, 119991 Moscow, Russia

ARTICLE INFO

ABSTRACT

In the present study, the Pulsed Laser Deposition (PLD) technique was applied to coat titanium for orthopaedic and dental implant applications. Calcium carbonate (CC) was used as starting coating material. The deposited CC films were transformed into octacalcium phosphate (OCP) by chemical treatments. The results of X-ray diffraction (XRD), Raman, Fourier Transform Infrared Spectroscopy (FTIR) and scanning electron microscopy (SEM) studies revealed that the final OCP thin films are formed on the titanium surface. Human myofibroblasts from peripheral vessels and the primary bone marrow mesenchymal stromal cells (BMMSs) were cultured on the investigated materials. It was shown that all the investigated samples had no short-term toxic effects on cells. The rate of division of myofibroblast cells growing on the surface and saturated BMMSs concentration for the OCP coating were about two times faster than of cells growing on the CC films.

1. Introduction

Titanium (Ti) implants are widely used for load bearing implants and inner fixation devices due to their relevant mechanical properties. Their integration with bone tissue depends on the physical-chemistry characteristics of the implant/tissue interface. Calcium phosphate coatings have been extensively applied in order to enhance the ability of the biomaterials to create bonds with the living host tissue [1]. Among calcium phosphate materials the better control of the integration process with bone tissue was provided by the hydroxyapatite (HA) coatings [2–4]. HA coatings have been extensively used in order to enhance the biological behaviour of implants and a number of deposition techniques have been developed and applied for this purpose during last two decades. They are utilized in most commercially available coated Ti implants. However, the deposition of dense, stoichiometric, and crystallised HA coating layers is frequently ineffective [5]. They have some disadvantages such as poor interfacial adhesion between coated Ti implants and host tissue and dramatic late implant failure [6].

During the last several years, growing attention has been brought to octacalcium phosphate (OCP) related to calcium phosphate materials [7]. OCP have been proposed as a possible precursor of the tooth enamel, dentine and bones in living organisms [8]. It has been reported that OCP pressed powders had high osteoconductive property when implanted in the sub-periosteal region of mouse calvaria [8,9]. Further, it has been demonstrated that OCP-based materials could stimulate osteoblastic cell differentiation in vitro [10,11] and had possibly osteotransductive properties, i.e. the capacity to provide new bone formation in vivo [7]. Therefore,

the use of OCP material for coatings could provide a sufficient potential to enhance the biological behaviour of Ti implants.

Only recently, a number of techniques for depositing OCP coatings on implants have been proposed for implant biofunctionalization [1,12–17]. It is well known that OCP is quite difficult to deposit by means of direct physical methods because its thermal decomposition takes place at low temperature. Most of the OCP coatings were deposited from supersaturated solutions and had a very low adhesion to the substrates [13–15]. Several attempts have been performed to deposit OCP on Ti substrate by Pulsed Laser Deposition (PLD) [16,17] and Matrix Assisted Pulsed Laser Evaporation techniques [1,12]. According to the X-ray diffraction (XRD) analysis, the coatings displayed an amorphous-poorly crystalline apatite structure.

The main concept of the present study is based on PLD combined with the biomimetic approach, avoiding a direct OCP deposition. We performed first the PLD coating of Ti surface by calcium carbonate (CC), followed by the chemical treatment of the coated surface in solutions. CC has been suggested as possible precursor for biomaterials [18]. In the field of biomineralization of CC, it provides a system to allow nucleation and growth of inorganic minerals including calcium phosphates at physiological conditions. In the present manuscript the formation of OCP on CC film was invented. Structural and morphological properties of the obtained films were investigated by XRD, Raman measurements and scanning electron microscopy (SEM). In addition, adhesion and *in vitro* tests were carried out. This work is the successful attempt to produce OCP coatings for biomedical applications, applying a physical deposition method − PLD to deposit CC film with following chemical treatment to obtain OCP coating.

2. Experimental section

2.1. Target preparation

For synthesis of starting CC powder, 30 g of CaO (Cat. No: 1305−78−8, Sigma-Aldrich), 62 g of $(NH_4)_2CO_3$ (Cat. No: 506−87−6, Sigma-Aldrich), and 300 mL of distilled water were added to a vessel for grinding, carried out for 30 min at room temperature. After filtration, powders were washed and dried at 80 °C for 24 h. CC pellet-target (diameter of 1 cm and thickness of 0,5 cm) was prepared by uniaxial pressing at 100 MPa.

2.2. Pulsed Laser Deposition

Thin films were deposited onto titanium substrates by PLD technique, using a Nd:YAG laser source (Handy YAG-Quanta System, $\lambda = 532$ nm, $\tau = 7$ ns, 10 Hz). The laser beam, oriented with an inclination of 45° with respect to the target surface, is focused by a lens system. The pure Ti substrates (1×1 cm^2 squares of 3 mm of thickness) were sandblasted with a 60-grid SiC abrasive powder. Before depositions, the substrates were boiled in aqua regia for 30 min, in order to remove any contaminant from the surface. During depositions, the Ti substrates were kept at room temperature. The CC targets were supported onto a rotating holder, in order to minimize laser induced craterization effect. The target-substrate distance was kept at 2 cm, for a deposition time of 5 h. The laser fluence was fixed at 30 J/cm^2.

2.3. Chemical treatment: preparation of octacalcium phosphate coatings

In order to transform the CC coatings into OCP, the procedure described elsewhere has been followed [7]. Briefly, an aqueous solution was prepared by dissolving of 115 g of $NH_4H_2PO_4$ (Cat. No:

7722−76−1, Sigma-Aldrich) in 500 mL of distilled water at room temperature, pH 4.1 ± 0.1. The CC coated Ti substrates were placed into the solution and were shaken in a sealed glass vessel for 168 h at 40 °C. After that, the coated Ti substrates were thoroughly washed in distilled water at least 5 times and dried overnight at 37 °C. Then, the obtained samples were placed in a second solution. The second solution was prepared by dissolving 95.2 g of CH$_3$COONa (Cat. No: 127−09−3, Sigma-Aldrich) in 700 mL of distilled water at 40 °C and pH 8.2 ± 0.2. The so-obtained samples were again shaken in a sealed glass vessel for 168 h at 40 °C. Finally, they were thoroughly washed in distilled water at least 5 times and dried overnight at 37 °C.

2.4. Characterization of octacalcium phosphate coating

Phase composition was analyzed by conventional XRD technique (X'Pert Pro MPD diffractometer, PANalytical, Netherlands). The XRD pattern has been obtained using the CuKα radiation ($\lambda = 1.54184$ Å) and performing the scan in 2 theta(θ) mode, keeping the incidence angle at 1.5°. A 0.03125° divergence slit on the incident beam path has been used and the 2θ scan step size was 0.02°. The phase analysis of the obtained pattern has been performed using the PANalytical High Score Plus software package. Micro-Raman measurements were carried out in backscattering configuration by a HORIBA LabRam 800 HR apparatus (HORIBA Scientific, Japan) equipped with an edge filter, two gratings (600 lines/mm and 1800 lines/mm). Excitation was performed with 632.8 nm radiation form a He-Ne laser source. The laser spot size impinging on the samples surface was about 5 μm in diameter when the 100x microscope objective was used. The spectrometer is connected to a Peltier cooled CCD detector. A spectral resolution of about 4 cm^{-1} was obtained by the holographic grating with 600 lines/mm. Fourier Transform Infrared Spectroscopy (FTIR) investigation was carried out using an IR microscope (Nicolet Avatar 330 FTIR spectrometer, England) in transmission mode. The microscope provides a control stage movement, aperture setting and focusing directly from the PC screen. Before FTIR analyses coatings was removed from titanium surface and mixed 1 mg of sample with 300 mg of KBr powder, followed by compacting those into a thin pellet in a stainless steel die of 1 cm inner diameter. FTIR data were recorded over the range of 4000 to 400 cm^{-1} with 128 scans. The morphology of samples was investigated using a Carl Zeiss NVision 40 high resolution Scanning Electron Microscope (SEM), equipped with an Oxford Instruments X-Max energy dispersive detector (80 mm^2) (Germany). The images were obtained at 1 kV acceleration voltage (SE2, magnifications up to ×100 k). The samples were analyzed by SEM without deposition of a conductive surface layer. Finally, the adhesive bonding strength of the obtained coatings was determined according to the ASTM C633-79 standard. A universal testing system, Instron 4204 (UK), was used for the adhesive strength measurement with a tensile speed of 1 mm/min. Five samples were tested to get an average value.

2.5. Cell culture

Prior to *in vitro* test, the samples were sterilized by heating at 120 °C for 2 h [7]. Afterwards, they were placed in the wells of 12 well plates (Greiner, Germany), one sample in the hole. After that, the wells were filled with culture medium Dulbecco''s modified Eagle's medium (DMEM) (Sigma-Aldrich, USA) plus 10% fetal calf serum (Gibco, USA). Gentamicin sulphate, up to a final concentration of 0.7 mM (Mosagrogen, Russia), was introduced into the culture medium, in order to assure the coefficient of molar absorption of $\varepsilon_{256} = 530$ l/mol. Then, the cells seeding on the material sample surface was performed at a concentration of 5×10^3 cells/

cm^2. In this work, the myofibroblasts from human peripheral vessels kindly provided by Prof. Vladimir S. Akatov, Institute of Theoretical and Experimental Biophysics, Russian Academy of Sciences, were used. Myofibroblasts were grown in CO_2-incubator at fully humidified atmosphere at 37 °C, 5% CO_2 and 95% room air at 96 h after treatment [19].

Analysis of cell's activity was performed using a fluorescence microscope DM 6000 (Leica, Germany). Analysis of mitotic activity was performed using *in vitro* staining of cells with fluorescent nuclear dye Hoechst 33342 (Sigma-Aldrich, USA). Mitotic cells revealed the distribution of chromatin, characteristic of prophase, metaphase, anaphase and telophase. For the analysis, at least 500 cells were counted. The mitotic index (MI) was calculated by the formula MI = (P + M + A + T)/N*100%, where (P + M + A + T) — the amount of cells at the stage of prophase, metaphase, anaphase and telophase, respectively, and N is the total number of analyzed cells.

To determine the number of alive and dead cells, the staining of cells growing on the sample surface with a fluorescent dye by kalayna AM (Sigma-Aldrich, USA) (2 µM) and propidium iodide (Sigma-Aldrich, USA) (2 µg/mL) was performed. Samples were treated with dye for 40 min at 37 °C. For the analysis, at least 500 cells were counted.

To obtain the cells were fixed on the material's surface in 4% paraformaldehyde (4 °C, 16 h). After fixation, the cells were washed three times with cold phosphate-saline buffer, then permeability using 0.5% solution of saponin (Sigma-Aldrich, USA). After triple washing in phosphate-buffered saline, the preparations were stained in acridine orange (Sigma-Aldrich, USA) (2 µg/mL) for 10 min.

Since this study would be to develop a Ti implant surface for orthopedics or dentistry in the aspect of biologically functional bone/material interface, presenting results of the proliferation of the primary bone marrow mesenchymal stromal cells (BMMSs) culture in addition to the mitotic activity of cells was considered. BMMSs culture was established by placing 3 mL of bone marrow aspirate from the femora and tibiae of adult rats (180−200 g) in 25 cm^2 culture flasks in advMEM (Invitrogen, USA) supplemented with 10% fetal bovine serum (FBS) (HyClone, USA). At confluence, the primary cells were trypsinized with 0.05% trypsin/EDTA solution (Invitrogen, USA) and passaged. A fluorescein diacetate (FDA) (Invitrogen, USA) viability probe assay was performed to estimate the proliferation of the investigated materials. BMMSs were seeded at a density of 10^5 cells/well in 12 well plates in DMEM supplemented with 10% FBS and cultured over 18 h. Then, the investigated samples were added to the cells. After 72 h, FDA with a concentration of 2 µL/ml was added to each well for 5 min. The fluorescence was measured by SpectraMax M5 Multi-Mode Microplate Reader (Molecular Devices, USA).

2.6. Statistical analysis

The research results are presented as means and standard error of the means. Significant differences for experimental data for the proliferative activity of myofibroblasts and BMMSs on Ti substrates, CC and OCP films were assessed using the ANOVA. All the experiments were performed with at least five repetitions.

3. Results and discussion

The XRD analysis (see Fig. 1 [1]) testified that the deposited coatings are composed of $CaCO_3$ (calcite, 100% peak at 2theta = 29.5 (PDF card no. 72-1652 [20])). No additional peaks, apart those of the Ti substrate (PDF card no. 05-0682 [20]), were registered. To confirm XRD data, Raman measurements were carried out for CC

target and −coating. Raman spectrum of CC target, shown in Fig. 2 (lower curve), is typical for polycrystalline calcite. The spectrum is dominated by the symmetric stretching mode of the carbonate ion at 1087 cm^{-1}, whereas peaks at 713 and 1437 cm^{-1} are related to in plane bending and antisymmetric stretching modes of carbonate ions. Signals at 152 and 281 cm^{-1} can be assigned to the calcite translational and rotational modes, in good agreement with the literature data [21]. Raman spectrum of the deposited films, presented in Fig. 2 (upper curve), is identical to that of the target, presenting the same crystalline structure of $CaCO_3$. Therefore, the application of PLD technique did not lead to the CC decomposition. The CC coating thickness, of the order of 10 µm, was adherent to Ti substrate and was quite uniform (Fig. 3, A).

The obtained CC films were transformed into dicalcium phosphate dihydrate (DCPD) ($CaHPO_4 \cdot 2H_2O$, Brushite) via a chemical soaking procedure in calcium nitrate solution for 168 h that it was confirmed by the conventional XRD (Fig. 1 [2]) (PDF card no. PDF 11-293 [20]). The overall conversion of CC to DCPD can be presented by the reaction given below.

$$CaCO_3 + NaH_2PO_4 \cdot 2H_2O \rightarrow CaHPO_4 \cdot 2H_2O + HCO_3^- + Na^+ \qquad (1)$$

FTIR spectra of DCPD films were exhibited the principal characteristic of DCPD (Fig. 4 (upper curve)). Namely, bands for the ν_4 bending vibrations of the P—O mode at 433, 530 and 580 cm^{-1} were observed. Bands at 873 and 1212 cm^{-1} were attributed to the HPO_4^{2-} group of DCPD. The band at 987 cm^{-1} originates in the P—O(H) ν_1 symmetric stretching vibration of PO_4^{3-}. The band at 1067 cm^{-1} was attributed to the ν_3 vibration of the PO_4^{3-} group. A peak at 1134 cm^{-1} was assigned to the ν'_6 and ν''_6 degenerate stretch of HPO_4^{2-} ions [22]. Water molecules possess three internal vibration modes. These are the symmetric (ν_1) at 3480 cm^{-1} and antisymmetric (ν_3) at 3150, 3273 and 3532 cm^{-1} OH$^-$ stretching modes, and the H_2O bending vibration (ν_2) at 1729 and 1650 cm^{-1} [23] (Fig. 4 (upper curve)). SEM micrographs of both CC and DCPD films are shown in Fig. 5 (A-A1 and B-B1). Particle size of the initial CC was about few microns. The DCPD crystals had a plate morphology (i.e. different from the common flat-plate type). The width of the DCPD plates ranged of about 0.5−1.0 µm and their thickness was over the range of 50−100 nm (Fig. 5, B-B1). The morphology of DCPD crystals obtained by *Mandel* et al. [24] during the transformation of DCPD powders at 36.5 °C in Dulbecco's
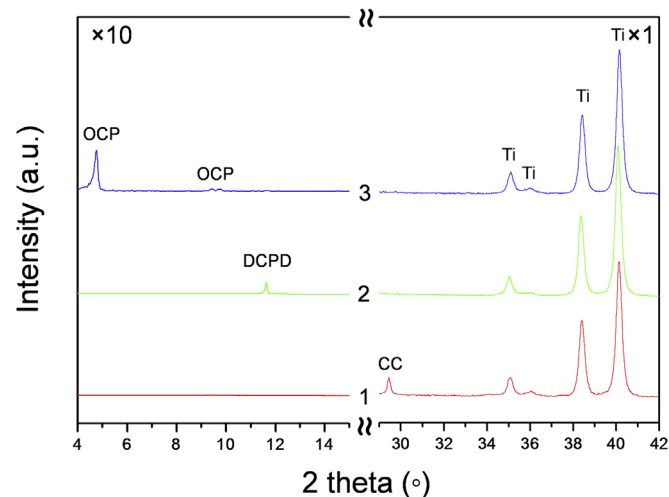

Fig. 1. XRD patterns of CC films (1); DCPD films (2) formed after CC soaking in calcium nitrate solution for 168 h and final OCP films (3) formed after DCPD soaking in sodium acetate for 168 h.
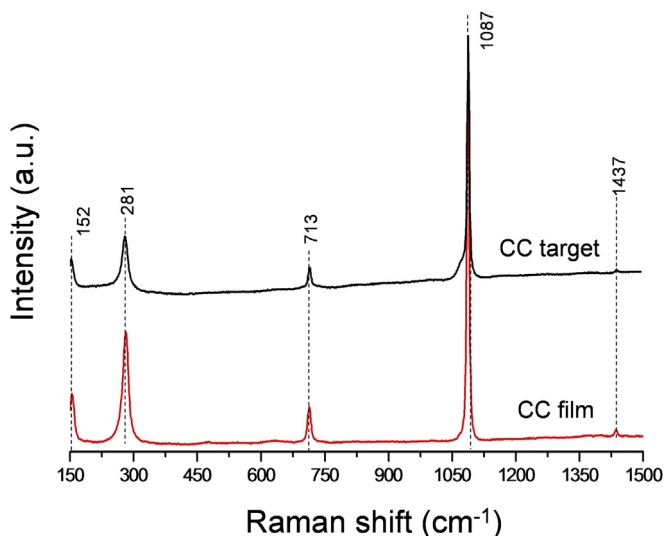
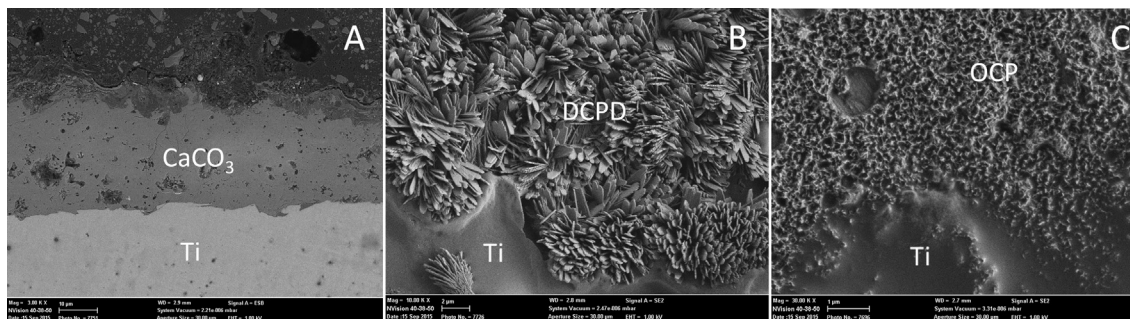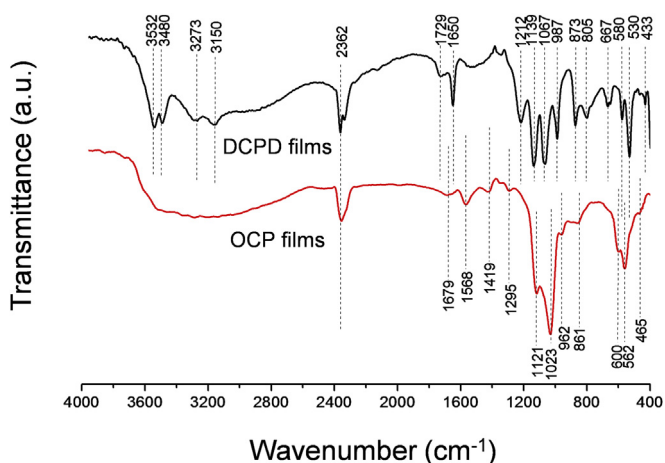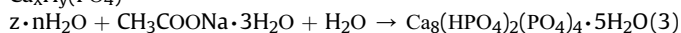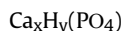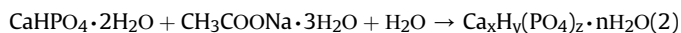**Fig. 2.** Raman spectrum of CaCO$_3$ target (lower curve) and of films deposited on Ti substrates (upper curve).

stacked DCPD water lilies, gradually formed in the place of the original template. On the other hand, this leads to intense dissolution thick PLD coating in front of the substrate surface. A lesser thickness of DCPD films was observed (~2 μm) (Fig. 3, B).

Further, the obtained DCPD films were transformed into OCP upon 168 h of soaking in sodium acetate, as shown by the XRD of Fig. 1 [3]. The overall conversion of DCPD to OCP can be visualised by the reactions:

$$CaHPO_4 \cdot 2H_2O + CH_3COONa \cdot 3H_2O + H_2O \rightarrow Ca_xH_y(PO_4)_z \cdot nH_2O \quad (2)$$

$$Ca_xH_y(PO_4)$$
$$z \cdot nH_2O + CH_3COONa \cdot 3H_2O + H_2O \rightarrow Ca_8(HPO_4)_2(PO_4)_4 \cdot 5H_2O \quad (3)$$

XRD of the films confirmed that they are mainly composed of the OCP phase (100) reflection at $2\theta = 4.9°$ (PDF card no. 026-1056 [20]). Some presence of unreacted CC or DCPD after 168 h of soaking in sodium acetate was observed (data not shown). The intense and well-resolved diffraction peaks indicate on crystallinity of the OCP films. In the literature [16], the XRD pattern of OCP coatings deposited on Ti substrates by means of PLD was reported

Fig. 3. SEM images of the cross section of CC films (A); DCPD films (B) formed after CC soaking in calcium nitrate solution for 168 h and final OCP films (C) formed after DCPD soaking in sodium acetate for 168 h.

Fig. 4. FTIR spectra of DCPD (upper curve) and OCP films (lower curve).

to display just a shoulder at about $2\theta = 4.7°$. In this work, the formed OCP crystals had the form of meshwork (Fig. 5, C-C1). The final OCP films were less than 1 μm thick (Fig. 3, C).

FTIR data of the OCP films are shown in Fig. 4 (lower curve), and are in good agreement with those previously reported by *Mandel* et al. [24] and *Fowler* et al. [25]. H–O–H or crystalline water of OCP was attributed to the wide band recorded over the range of 3700-2800 cm^{-1}. The OH$^-$ bending modes originating from the HPO$_4^{2-}$ groups of OCP were observed at 1295 cm^{-1}. P–O in HPO$_4^{2-}$ and PO$_4^{3-}$ groups were assigned at 1121, 1023, 962, 600 and 562 cm^{-1}. The P–OH stretching mode of HPO$_4^{2-}$ groups was at 861 cm^{-1}. Finally, the FTIR spectra of both DCPD and OCP films has some amount of CO$_3^{2-}$ group, which is proven by presence the absorption band at 2362 cm^{-1} and within the range between 1600 and 1400 cm^{-1} [26].

The standard adhesion tests shown that about 90% of the OCP coating was well attached to the Ti substrate, indicating sufficient mechanical properties.

All the investigated samples did not show any cytotoxic effect *versus* myofibroblasts from human peripheral vessels, when cultured for 3 days. The DCPD films were not investigated due to the unsuitable pH value 4.1 ± 0.1. In the case of Ti, the number of living cells was 96 ± 2%, whereas for CC and OCP films − 94 ± 4% and 98 ± 1%, respectively. It should be noted that by culturing cells on the standard plastic culture plate under the same conditions over 3 days, there were about 97 ± 2% of living cells. Thus, all the
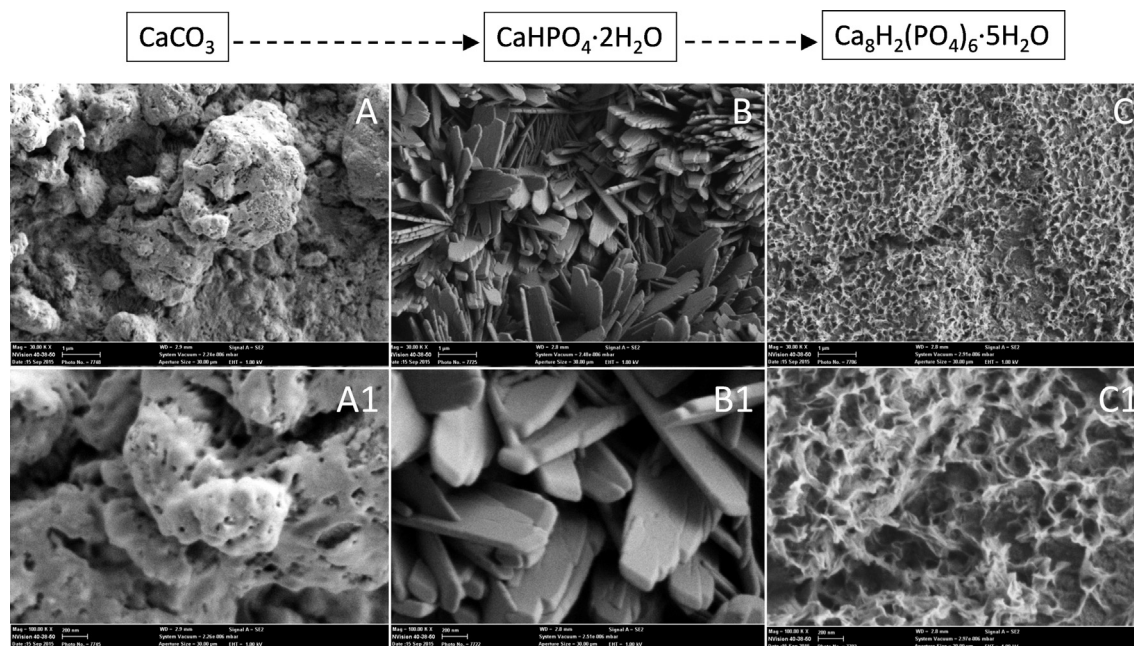
Modified Eagle Medium solutions was quite similar to those shown in Fig. 5, B-B1. In the present work calcium carbonate particles were chemically attacked by the acidic H$_2$PO$_4^-$ ions in the solution, this process followed by a template synthesis-type reaction. The PLD deposited CC films behaved as the template for the dumbbells of

$$CaCO_3 \dashrightarrow CaHPO_4 \cdot 2H_2O \dashrightarrow Ca_8H_2(PO_4)_6 \cdot 5H_2O$$

Fig. 5. SEM images of (A–A1) CC, (B–B1) DCPD (after soaking in calcium nitrate solution at 168 h) and (C–C1) OCP (after soaking in sodium acetate at 168 h) films.

investigated samples had no short-term toxic effects on cells.

In addition to cytotoxic properties, the indicator of the proliferative activity of myofibroblasts on the surfaces of the tested materials was measured (Fig. 6). It is shown that the Mitotic Index (MI) of cells growing on the Ti surface was about 5.6%, for CC films — 2.8% and OCP films — 6.9%, respectively. By culturing cells on the plastic culture plate under the same conditions, the MI reaches 6.5%. The MI of cells growing on the CC film surface of about 3.0% indicates a significantly lower rate of cell proliferation.

Micrographs of fluorescent images of myofibroblasts from human peripheral vessels on the surface of the investigated materials are presented in Fig. 7. It is shown that the pure titanium and OCP films (Fig. 7, A and C) are quite suitable for cell's attachment and spreading with respect to the CC films (Fig. 7, B). Cells growing on the surface of the CC films for 3 days, in contrast to OCP films, did not colonize the entire available surface and did not form a confluent monolayer. After 96 h, the cells occupy only about 70% of the available surface of CC films, whereas confluent monolayers are observed on pure Ti and OCP films after 70 and 55 h, respectively. By culturing cells on plastic culture plate under the same conditions the formation of monolayer is observed after 60 h. Further BMMSs proliferation was studied. The saturated cell concentration was about 6×10^4, 4×10^4 and 8×10^4 for pure Ti, CC and OCP films (Fig. 8).

The data showed that OCP films had a higher proliferation rate for both myofibroblasts and BMMSs than that of CC films. The high Ca^{2+} concentration due to the fast resorption rate of $CaCO_3$ can decreased the proliferation rate of CC films for both myofibroblasts and BMMSs. The data in agreement with *Liu* et al. [27], which demonstrate that CC coated Ti reduces the initial attachment/proliferation of osteoblastic cells. The positive effect of OCP on different cells type proliferation in comparison to HA and tricalcium phosphate was observed in numerous studies [28–31]. The possible mechanism such enhanced behaviour proposed by *Suzuki* [28] and included the process of OCP to HA conversion, which induces physicochemical changes, including Ca^{2+} consumption and inorganic phosphate ions release.
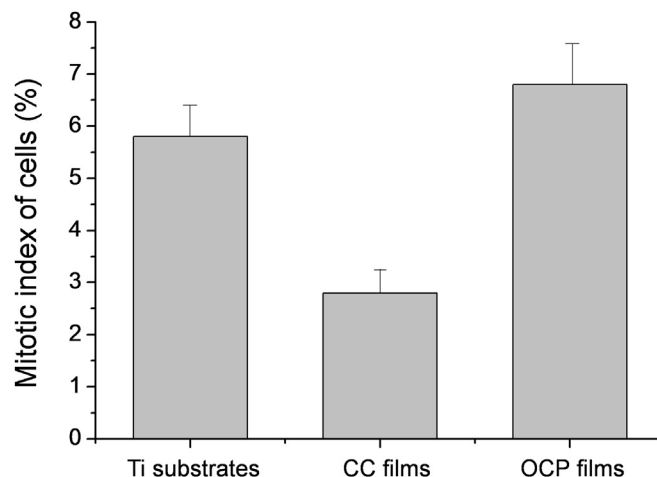

Fig. 6. Proliferative activity of myofibroblasts on Ti substrates, CC films and OCP films.

To summarize, the results of this work showed that in order to obtain OCP films on Ti, the direct PLD deposition of CC on Ti substrate, followed by chemical treatments of coatings in solutions, is a suitable alternative to more complex PLD [16,17] and Matrix Assisted Pulsed Laser Evaporation procedures [1,12]. *In vivo* tests of OCP films on Ti are planned in order to assess their biological behaviour.

4. Conclusion

A method to produce OCP films on the Ti substrates was developed in this work. First, the PLD technique was applied to deposit $CaCO_3$ coatings on Ti. Subsequent chemical treatments of the deposited coatings in solutions led to their chemical transformation first into DCPD and then into OCP. The prepared films are uniform, continuous, without cracks and show good adhesion to the Ti substrate. To test the cytotoxic properties, myofibroblast cells
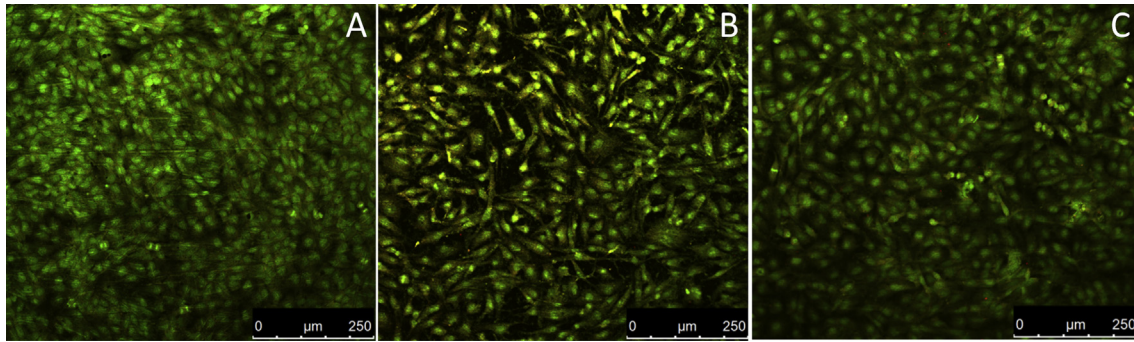
Fig. 7. Micrographs of fluorescent images of myofibroblasts from human peripheral vessels on Ti substrates (A), CC films (B) and OCP films (C).
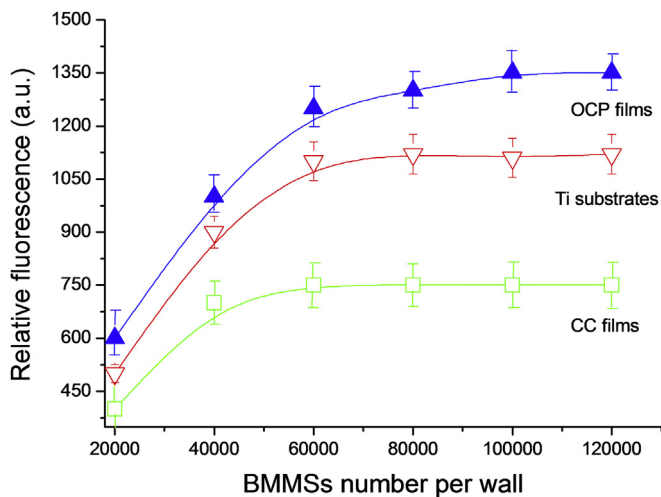

Fig. 8. BMMSs saturation curves measured by FDA fluorescence for Ti substrates, CC films and OCP films.

from human peripheral vessels were cultured for 3 days on the films surface. The number of living cells on OCP films was 98 ± 1%. The MI index of the proliferative activity of myofibroblasts on the OCP surfaces was measured to be 6.9%. It was shown that the OCP films are more suitable for attachment and spreading of cells with respect to Ti substrates and CC films, e.g. colonizing the entire available surface and forming a confluent monolayer after 55 h. Moreover, OCP films had a higher proliferation rate for both myofibroblasts and BMMSs. Therefore, OCP coating on the titanium surface could provide a favorable implant microenvironment for osseointegration in clinical practies.

Conflict of interest statement

The authors declare that the research was conducted in the absence of any commercial or financial relationships that could be construed as a potential conflict of interest.

Acknowledgments

References

[1] E. Boanini, P. Torricelli, L. Forte, S. Pagani, N. Mihailescu, C. Ristoscu, I.N. Mihailescu, A. Bigi, Antiresorption implant coatings based on calcium alendronate and octacalcium phosphate deposited by Matrix assisted pulsed laser evaporation colloids and surfaces, J. Biointerfaces 136 (2015) 446–456.

[2] R.I.M. Asri, W.S.W. Harun, M.A. Hassan, S.A.C. Ghani, Z. Buyong, A review of hydroxyapatite-based coating techniques: sol–gel and electrochemical depositions on biocompatible metals, J. Mech. Behav. Bio. Mater. 57 (2016) 95–108.

[3] M.S. Bryington, M. Hayashi, Y. Kozai, S. Vandeweghe, M. Andersson, A. Wennerberg, R. Jimbo, The influence of nano hydroxyapatite coating on osseointegration after extended healing periods, J. Dent. Mater. 29 (2013) 514–520.

[4] J.V. Rau, A. Generosi, S. Laureti, V.S. Komlev, D. Ferro, S.N. Cesaro, B. Paci, V.R. Albertini, E. Agostinelli, S.M. Barinov, Physicochemical investigation of pulsed laser deposited carbonated hydroxyapatite films on titanium, ACS Appl. Mater. Interfaces 1 (8) (2009) 1813–1820.

[5] Robert B. Heimann The challenge and promise of low-temperature bioceramic coatings: an editorial doi: http://doi.org/10.1016/j.surfcoat.2015.12.082.

[6] E. Mohseni, E. Zalnezhad, A.R. Bushroa, Comparative investigation on the adhesion of hydroxyapatite coating on Ti–6Al–4V implant: a review paper, Int. J. Adhes. Adhes. 48 (2014) 238–257.

[7] V.S. Komlev, S.M. Barinov, I.I. Bozo, R.V. Deev, I.I. Eremin, A. Yu. Fedotov, A.N. Gurin, N.V. Khromova, P.B. Kopnin, E.A. Kuvshinova, V.E. Mamonov, V.A. Rybko, N.S. Sergeeva, A. Yu. Teterina, V.L. Zorin, Bioceramics composed of octacalcium phosphate demonstrate enhanced biological behavior, ACS Appl. Mater. Interfaces 6 (19) (2014) 16610–16620.

[8] O. Suzuki, M. Nakamura, Y. Miyasaka, M. Kagayama, M. Sakurai, bone formation on synthetic precursors of hydroxyapatite, J. Exp. Med. 164 (1991) 37–50.

[9] O. Suzuki, M. Nakamura, Y. Miyasaka, M. Kagayama, M. Sakurai, Maclura pomifera agglutinin-binding glycoconjugates on converted apatite from synthetic octacalcium phosphate implanted into subperiosteal region of mouse calvaria, Bone Min. 20 (1993) 151–166.

[10] R.M. Shelton, Y. Liu, P.R. Cooper, U. Gbureck, M.J. German, J.E. Barralet, Bone marrow cell gene expression and tissue construct assembly using octacalcium phosphate microscaffolds, Biomaterials 27 (2006) 2874–2881.

[11] Y. Liu, P.R. Cooper, J.E. Barralet, R.M. Shelton, Influence of calcium phosphate crystal assemblies on the proliferation and osteogenic gene expression of rat bone marrow stromal cells, Biomaterials 28 (2007) 1393–1403.

[12] E. Boanini, P. Torricelli, M. Fini, F. Sima, N. Serban, I.N. Mihailescu, A. Bigi, Magnesium and strontium doped octacalcium phosphate thin films by Matrix assisted pulsed laser evaporation, J. Inorg. Biochem. 1 (2012) 65–72.

[13] L. Bao, J. Liu, F. Shi, Y. Jiang, G. Liu, Preparation and characterization of TiO2 and Si-doped octacalcium phosphate composite coatings on zirconia ceramics (Y-TZP) for dental implant applications, Appl. Surf. Sci. 290 (2014) 48–52.

[14] A.A. Ribeiro, R.M. Balestra, M.N. Rocha, S.B. Peripolli, M.C. Andrade, L.C. Pereira, M.V. Oliveira, Dense and porous titanium substrates with a biomimetic calcium phosphate coating, Appl. Surf. Sci. 265 (2013) 250–256.

[15] M. Stefanic, K. Krnel, I. Pribosic, T. Kosmac, Rapid biomimetic deposition of octacalcium phosphate coatings on zirconia ceramics (Y-TZP) for dental implant applications, Appl. Surf. Sci. 10 (258) (2012) 4649–4656.

[16] G. Socol, P. Torricelli, B. Bracci, M. Iliescu, F. Miroiu, A. Bigi, J. Werckmann, I.N. Mihailescu, Biocompatible nanocrystalline octacalcium phosphate thin films obtained by pulsed laser deposition, Biomaterials 25 (2004) 2539–2545.

[17] A. Bigi, B. Bracci, F. Cuisinier, R. Elkaim, M. Fini, I. Mayer, I.N. Mihailescu, G. Socol, L. Sturba, P. Torricelli, Human osteoblast response to pulsed laser deposited calcium phosphate coatings, Biomaterials 26 (2005) 2381–2389.

[18] S. Rokidi, C. Combes, P.G. Koutsoukos, The calcium phosphate-calcium carbonate system: growth of octacalcium phosphate on calcium carbonates, Cryst. Growth Des. 11 (2011) 1683–1688.

[19] S.A. Garmash, V.S. Smirnova, O.E. Karp, A.M. Usacheva, A.V. Berezhnov, V.E. Ivanov, A.V. Chernikov, V.I. Bruskov, S.V. Gudkov, Pro-oxidative, genotoxic and cytotoxic properties of uranyl ions, J. Environ. Radioact. 127 (2014) 163–170.

[20] International Centre for Diffraction Data, Database JCPDS, 2001.

[21] M. De La Pierre, C. Carteret, L. Maschio, E. André, R. Orlando, R. Dovesi, The raman spectrum of $CaCO_3$ polymorphs calcite and aragonite: a combined experimental and computational study, J. Chem. Phys. 140 (2014) 164509.

[22] S. Singh, V. Singh, S. Aggarwal, U.K. Mandal, Synthesis of brushite nanoparticles at different temperatures, Chem. Papers 64 (2010) 491–498.

[23] A. Hirsch, I. Azuri, L. Addadi, S. Weiner, K. Yang, S. Curtarolo, L. Kronik, Infrared absorption spectrum of brushite from first principles, Chem. Mater. 26 (2014) 2934–2942.

[24] S. Mandel, A.C. Tas, Brushite ($CaHPO_4 \cdot 2H_2O$) to octacalcium phosphate ($Ca_8(HPO_4)_2(PO_4)_4 \cdot 5H_2O$) transformation in DMEM solutions at 36.5 °C, Mater. Sci. Eng. C 30 (2010) 245–254.

[25] B.O. Fowler, M. Marković, W.E. Brown, Octacalcium phosphate. 3. Infrared and raman vibrational spectra, Chem. Mater. 5 (1993) 1417–1423.

[26] L. Berzina-Cimdina, N. Borodajenko, Research of calcium phosphates using fourier transform infrared spectroscopy, infrared spectroscopy, in: T. Theophile (Ed.), Materials Science, Engineering and Technology, InTech, Rijeka, Croatia, 2012, pp. 123–148.

[27] Y. Liu, T. Jiang, Y. Zhou, Z. Zhang, Z. Wang, H. Tong, X. Shen, Y. Wang, Evaluation of the attachment, proliferation, and differentiation of osteoblast on a calcium carbonate coating on titanium surface, Mater Sci. Eng. C 31 (2011) 1055–1061.

[28] O. Suzuki, Octacalcium phosphate (OCP)-based bone substitute materials, Jpn. Dent. Sci. Rev. 49 (2013) 58–71.

[29] V.L. Zorin, V.S. Komlev, A.I. Zorina, N.V. Khromova, E.V. Solovieva, A.Y. Fedotov, I.I. Eremin, P.B. Kopnin, Octacalcium phosphate ceramics combined with gingiva-derived stromal cells for engineered functional bone grafts, Biomed. Mater 9 (2014) 055005.

[30] O. Suzuki, S. Kamakura, T. Katagiri, Surface chemistry and biological responses to synthetic octacalcium phosphate, J. Biomed. Mater Res. B Appl. Biomater. 77 (2006) 201–212.

[31] P. Jiang, J. Liang, R. Song, Y. Zhang, L. Ren, L. Zhang, P. Tang, C. Lin, Effect of octacalcium-phosphate-modified micro/nanostructured titania surfaces on osteoblast response, ACS Appl. Mater. Interfaces 7 (2015) 14384–14396.